

**Brain clock driven by neuropeptides and second messengers**Jesus Miro-Bueno<sup>1,\*</sup> and Petr Sosík<sup>1,2,†</sup><sup>1</sup>*Research Institute of the IT4Innovations Centre of Excellence, Faculty of Philosophy and Science, Silesian University in Opava, 74601 Opava, Czech Republic*<sup>2</sup>*Departamento de Inteligencia Artificial, Escuela Técnica Superior de Ingenieros Informáticos, Universidad Politécnica de Madrid, Madrid, Spain*

(Received 18 February 2014; revised manuscript received 20 August 2014; published 9 September 2014)

The master circadian pacemaker in mammals is localized in a small portion of the brain called the suprachiasmatic nucleus (SCN). It is unclear how the SCN produces circadian rhythms. A common interpretation is that the SCN produces oscillations through the coupling of genetic oscillators in the neurons. The coupling is effected by a network of neuropeptides and second messengers. This network is crucial for the correct function of the SCN. However, models that study a possible oscillatory behavior of the network itself have received little attention. Here we propose and analyze a model to examine this oscillatory potential. We show that an intercellular oscillator emerges in the SCN as a result of the neuropeptide and second messenger dynamics. We find that this intercellular clock can produce circadian rhythms by itself with and without genetic clocks. We also found that the model is robust to perturbation of parameters and can be entrained by light-dark cycles.

DOI: [10.1103/PhysRevE.90.032705](https://doi.org/10.1103/PhysRevE.90.032705)

PACS number(s): 87.18.Yt, 82.39.Rt, 87.19.lj

**I. INTRODUCTION**

The mammalian brain contains a master clock in a small region called the suprachiasmatic nucleus (SCN) [1,2]. This master pacemaker produces rhythms with a circadian (24 hour) period. The master clock regulates essential functions such as cell cycle, metabolism, signaling, hormone secretion, and body temperature. Disturbances in circadian rhythms can be related to cancer as well as neurodegenerative and sleep disorders [3,4]. Despite its important role in the regulation of crucial biological functions, it is still unclear how the SCN produces circadian rhythms. Clarifying the oscillatory mechanism of the SCN can be essential for obtaining a better understanding of the causes of many diseases and for finding more effective treatments to restore proper biological rhythms. The SCN is composed of about 20 000 neurons, each containing a genetic clock [5]. A genetic clock is a network of interconnected genes [6–13]. Connections between genes produce positive and negative feedback loops in the network, due to which the genes are expressed periodically [14]. The investigation of genetic clocks [15] and coupled oscillators [16] entrained by pacemakers is important for understanding the synchronization properties of the SCN. These genetic clocks are coupled by neurotransmitters in the SCN. A class of neurotransmitters called neuropeptides seems to be mainly involved in the coupling [1,2,5]. In addition to neuropeptides, the second messengers cAMP and Ca<sup>2+</sup> are crucial for coupling and the correct functioning of the SCN [17–22]. Second messengers stimulate the release of neuropeptides in neurons. In recent years it has been discovered that the genetic clocks produce damped and unstable oscillations in isolated neurons [23,24]. Nevertheless, the master clock still oscillates with these unstable genetic oscillators [5,23], indicating that connections among neurons are crucial to production of rhythms. SCN models with stable, damped, or highly disrupted genetic clocks

have been investigated [20,25–34]. However, the possible oscillatory behavior of the network of neuropeptides and second messengers has not been studied beyond its traditional coupling role. Here, we propose and study a mathematical and computational model to examine its oscillatory potential and clarify the underlying oscillatory mechanism in the SCN. We show that the neuronal network in the SCN can contain an intercellular clock that operates without genetic clocks. The dynamics of this intercellular clock is driven by neuropeptides and second messengers. First, we study the model without genetic oscillators; we find that the intercellular clock produces synchronized oscillations. Then we study the model including genetic clocks inside neurons. We find that the intercellular clock coupled with genetic clocks produces synchronized rhythms and, more importantly, the model predicts oscillations in the concentration of second messengers when genetic clocks are uncoupled. This prediction diverges from what would be expected of a master clock driven by genetic oscillators. Simple [6–10] and more detailed [11–13] models of genetic clocks have been investigated in the last few years. Here, we use a standard model that has been studied for circadian clocks in *Neurospora*, *Drosophila*, and mammals [35].

**II. MODEL**

Our model of the intercellular clock is a network of neuropeptides and second messengers (Fig. 1). Positive feedback loops are created by these neuropeptides and second messengers (cAMP and Ca<sup>2+</sup>) in the SCN [21]. The release of neuropeptides from a neuron is controlled by second messengers which in turn are controlled by incoming neuropeptides from other neurons. On the other hand, the action of neuropeptides is terminated by enzymatic degradations carried out by peptidases [36,37]. Simple models like this, with enzymatic reactions and positive feedbacks, can produce reliable oscillations [10,38].

We simulate 100 neurons with 400 connections in a local network. Each neuron is connected to its four neighbors in a two-dimensional (2D) square lattice with periodic boundary

\*jesus.mirobueno@fpf.slu.cz

†petr.sosik@fpf.slu.cz

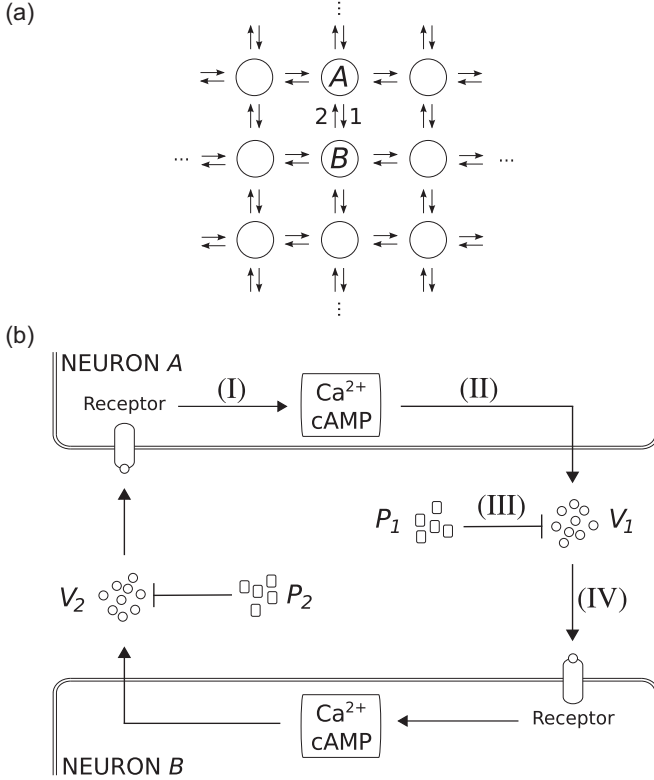
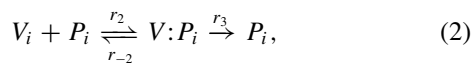
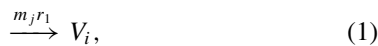


FIG. 1. Intercellular clock model of the SCN. (a) A local network. Each neuron is connected to its four neighbors in a 2D square lattice with periodic boundary conditions. The connection from neuron A to neuron B is denoted by 1 and the connection from B to A is denoted by 2. (b) A detailed model of the two connections between neurons A and B. Activated receptors in neuron A stimulate the synthesis and accumulation of second messengers (cAMP and  $\text{Ca}^{2+}$ ) (I). The second messengers modulate the release of neuropeptides  $V_1$  (II) in connection 1. The peptidases  $P_1$  degrade the neuropeptides  $V_1$  by an enzymatic reaction (III). The receptors of neuron B are activated by  $V_1$  (IV). In neuron B this activation triggers the same signaling as in neuron A. The signaling ends in the release of neuropeptides  $V_2$  and peptidases  $P_2$  in connection 2.

conditions (Fig. 1). The number of neurons and connections in the network are denoted as  $N$  and  $n$ , respectively. Note that the number of incoming and outgoing connections in the network are the same and equal to  $n$ . We use values for the parameters obtained from previous models, or within biologically plausible ranges (see Table SV [39]). The biochemical reactions that describe the intercellular clock are the following:



where  $V_i$  are the neuropeptides in the connection  $i$  and  $P_i$  are peptidases that degrade  $V_i$ . In (1)–(7) we use the following notation: the subscripts  $i$  and  $k$  are reserved for connections, and the subscripts  $j$  and  $l$  are reserved for neurons. Their values are  $i \in \{1, \dots, n\}$ ,  $j$  is the index of the neuron that releases  $V_i$

and  $P_i, k$  are indices of incoming connections to neuron  $j$ , and  $l \in \{1, \dots, N\}$ . The reactions for a simple example with three neurons and six connections are shown in Fig. S1 [39].

The dynamics of neuropeptides comprise two parts in a connection: release and degradation. We assume that a neuropeptide  $V_i$  is released in the connection  $i$  by a neuron  $j$  following the reaction (1), where  $r_1$  is the rate of the reaction. This rate is modulated by  $m_j$ , which represents the strength of the cAMP and  $\text{Ca}^{2+}$  signaling in neuron  $j$ . The factor  $m_j$  depends on incoming connections from other neurons and can be expressed as (see Appendix A)

$$m_j = \frac{m_0 K + F_j}{K + F_j}, \quad (4)$$

where  $K$  is the equilibrium dissociation constant,  $m_0$  is the minimum value of  $m_j$ , and  $F_j = \sum_k V_k$  is the total amount of released neuropeptides in neuron  $j$  from the incoming connections.  $V_k$  is the amount of neuropeptides released to neuron  $j$  in the connection  $k$ . The minimum and maximum values of  $m_j$  are  $m_0$  and 1, respectively. Note that second messengers increase the number of action potentials in SCN neurons, which in turn stimulate neuropeptide release [21]. In our model we assume that these two steps occur in a single step: second messengers stimulate neuropeptide release [26]. The neuropeptides released in the connection  $i$  are degraded by peptidases  $P_i$  following the enzymatic reaction (2) where  $r_2, r_{-2}$ , and  $r_3$  are the reaction rates, and  $V:P_i$  is the complex created by the binding of peptidases to neuropeptides. The dynamics of peptidases is described by simple production and degradation reactions (3) with rates  $r_4$  and  $r_5$ , respectively. We use stochastic modeling to study the dynamics of the model. Stochastic simulations take into account the random nature of chemical reactions in contrast to differential equations [42].

### III. RESULTS AND DISCUSSION

The simulation of the model shows that the amount of neuropeptides, peptidases, and the strength of the cAMP and  $\text{Ca}^{2+}$  signaling oscillate synchronously [Fig. 2(a)]. The period of the neuropeptide oscillations is about 24 hours and does not change with the size of the network [Fig. 2(b)]. We study the synchronization degree of the model as a function of the number of connections. Our model shows a transition from unsynchronized to synchronized oscillations when the number of connections is increased [Fig. 2(c)]. We use the so-called order parameter ( $O_p$ ) to measure the degree of synchrony over a time interval [43]. The  $O_p$  for neuropeptides  $V$  is the ratio of the variance of the mean number of  $V$  in all the connections to the mean variance of each individual connection in a time interval:

$$O_p = \frac{\langle \bar{V}^2 \rangle - \langle \bar{V} \rangle^2}{\frac{1}{n} \sum_{i=1}^n (\langle V_i^2 \rangle - \langle V_i \rangle^2)}$$

$$\bar{V} = \frac{1}{n} \sum_{i=1}^n V_i, \quad (5)$$

where brackets denote time average. Except if otherwise stated,  $O_p$  is calculated for neuropeptides. The  $O_p$  is particularly suitable for measuring the transition between unsynchronized

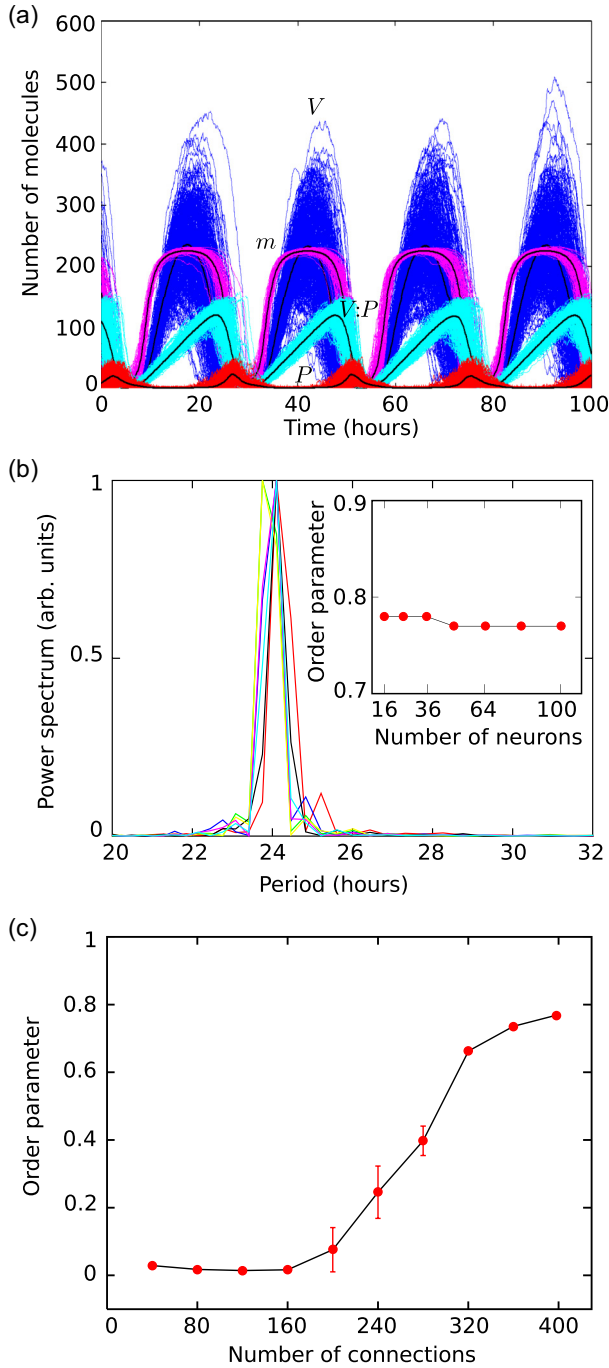


FIG. 2. (Color online) Simulations of the intercellular clock model. (a) Time evolution of the biomolecules involved in the 400 connections: neuropeptides ( $V$ , blue), peptidases ( $P$ , red), neuropeptide-peptidase complexes ( $V:P$ , cyan), and the strength of the cAMP and  $Ca^{2+}$  signaling ( $m$ , magenta, dimensionless, scaled by 250). Black lines represent the average. (b) Power spectrum and  $O_p$  (inset) for square lattices of 16, 25, 36, 49, 64, 81, and 100 neurons (64, 100, 144, 196, 256, 324, and 400 connections, respectively). Computed time for each lattice: 1000 hours. (c)  $O_p$  as a function of the number of connections for 100 neurons in a square lattice. Except if otherwise stated, we calculated the mean and standard deviation of the  $O_p$  for ten simulations (one simulation for 360 and 400 connections). Computed time for each simulation: 400 hours (see Table SV for parameter values [39]).

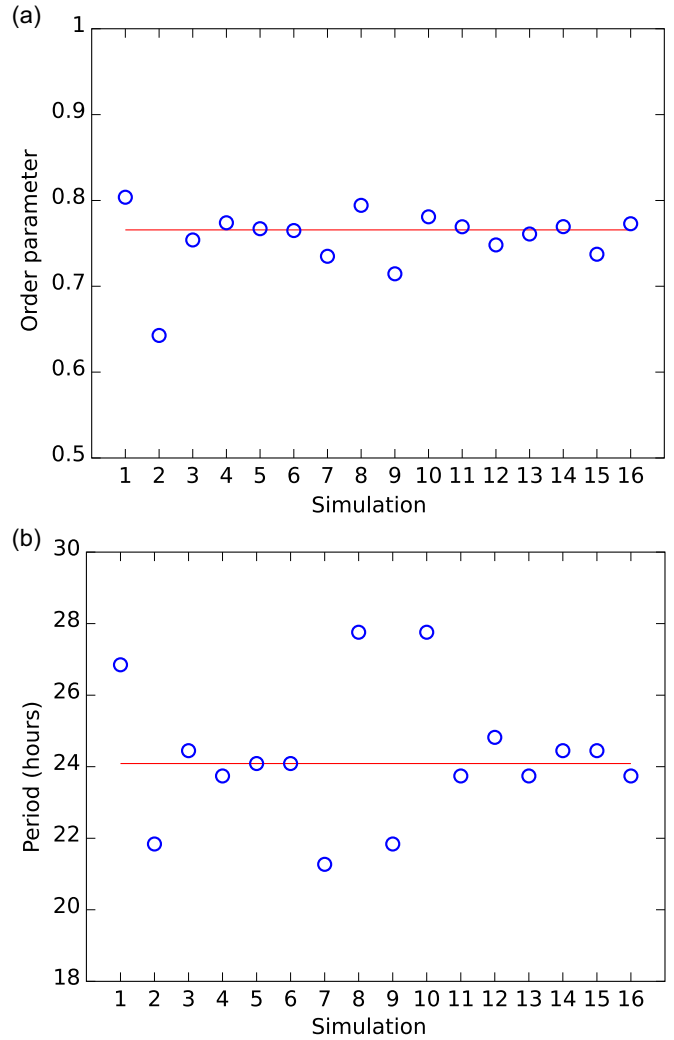


FIG. 3. (Color online) Model robustness to perturbation of parameters. The value was increased and decreased by 15% for each parameter [10,40] (in total: 16 simulations). (a) Robustness of the order parameter. (b) Robustness of the period. The 16 simulations are denoted in the  $x$  axis. Simulations 1, 2, 3, 4, 5, 6, 7, 8, 9, 10, 11, 12, 13, 14, 15, and 16 correspond to  $r_1^p = 1.15r_1$ ,  $r_1^p = 0.85r_1$ ,  $r_2^p = 1.15r_2$ ,  $r_2^p = 0.85r_2$ ,  $r_{-2}^p = 1.15r_{-2}$ ,  $r_{-2}^p = 0.85r_{-2}$ ,  $r_3^p = 1.15r_3$ ,  $r_3^p = 0.85r_3$ ,  $r_4^p = 1.15r_4$ ,  $r_4^p = 0.85r_4$ ,  $r_5^p = 1.15r_5$ ,  $r_5^p = 0.85r_5$ ,  $m_0^p = 1.15m_0$ ,  $m_0^p = 0.85m_0$ ,  $K^p = 1.15K$ , and  $K^p = 0.85K$ , respectively. The red lines denote the value of the order parameter and the period without perturbations. The superscript  $p$  denotes parameter perturbed. (Computed time for each simulation: 1000 hours.)

and synchronized oscillations. The values  $O_p = 0$  and  $O_p = 1$  correspond to unsynchronized and perfectly synchronized oscillations, respectively. In our case, the maximum value of  $O_p$  for synchronized oscillations is about 0.8. This value agrees with the results of previous models [26,29]. The maximum value of  $O_p$  is almost reached when the number of connections is about 320, corresponding to 80% of the total connections. This means that to obtain synchronized oscillations, the mean number of connections per neuron can be reduced from four to about three. We also found that the model is robust to perturbation of parameters (Fig. 3). The  $O_p$  is close to 0.8

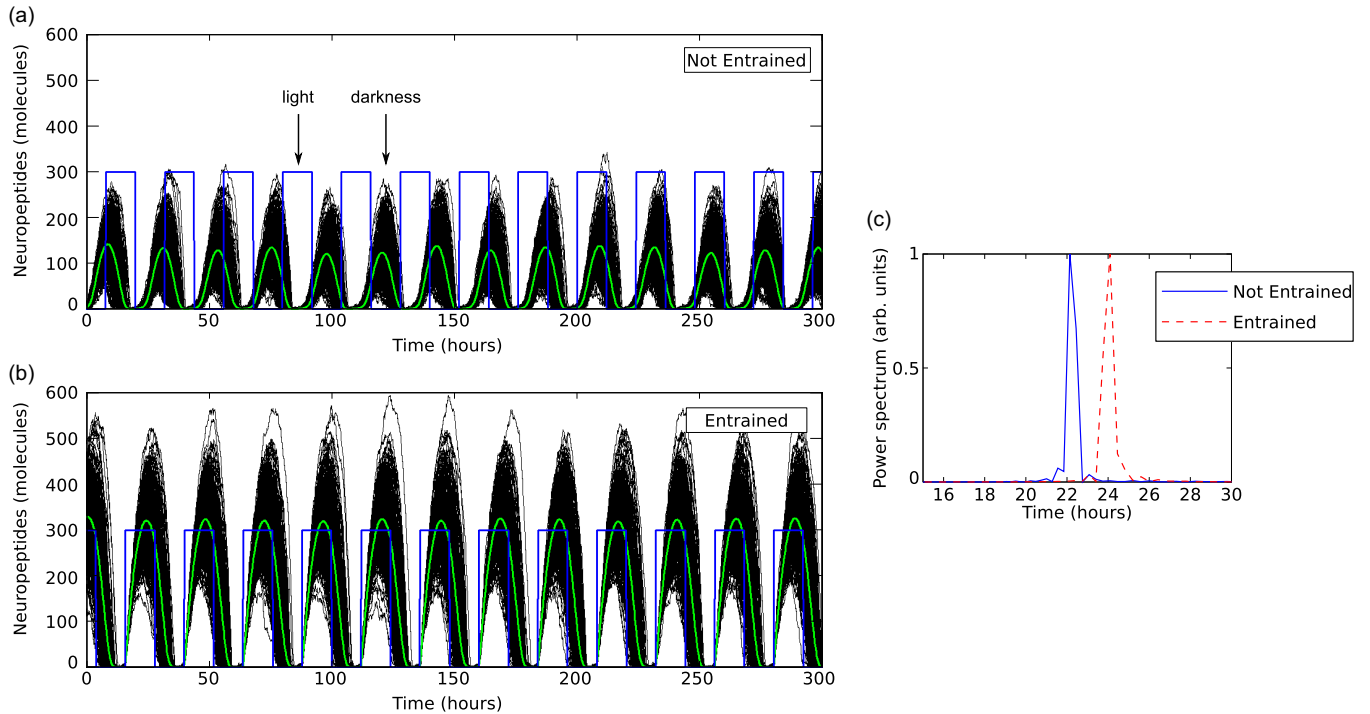


FIG. 4. (Color online) Entrainment of the intercellular clock by light-dark cycles (12 hours of light and 12 hours of darkness). (a) Time evolution of the neuropeptides without entrainment. (b) Time evolution of the neuropeptides with entrainment. Black and green (light gray) lines represent the neuropeptides and average, respectively. Blue lines (square wave form) represent the light-dark cycles. Light increases the amount of second messengers in SCN neurons [2,41]. Therefore, we assume that the strength of the second messenger signaling in the SCN is maximum with light, i.e.,  $m_j = 1$ . And during darkness,  $m_j$  follows Eq. (4). The rates are the same as in Table SV [39], but now  $r_1 = 90$  molecules  $\text{hour}^{-1}$  in order to produce oscillations with a period shorter than 24 hours [32]. (c) Power spectrum of average neuropeptides for (a) (blue line) and (b) (dashed red line). (Computed time for each simulation: 1000 hours.)

[Fig. 3(a)] and the changes in the period are less than 16% [Fig. 3(b)]. Specifically, the rates  $r_1$ ,  $r_3$ , and  $r_4$  are more sensitive to perturbation. Our model predicts that the period increases or decreases by more than 2 hours when these rates are increased or decreased. On the other hand, we demonstrate that the intercellular clock can be entrained by light-dark cycles like canonical genetic clocks (Fig. 4). Light increases the amount of second messengers during daytime [2]. We reduce the value of  $r_1$  in order to produce oscillations with a period shorter than 24 hours [32]. Then, the intercellular clock without entrainment does not oscillate in phase with light-dark cycles [Fig. 4(a)], but it does when it is entrained [Fig. 4(b)]. The period of the entrained oscillations is increased to 24 hours [Fig. 4(c)].

Next, we demonstrate that our model makes predictions that diverge from what would be expected of a SCN driven by genetic clocks. We compare two simulations of wild-type and mutant SCN (Fig. 5). In the first simulation the network is only composed of wild-type neurons [Fig. 5(a)]. Each neuron contains a genetic clock that is coupled with the intercellular clock. The details of the genetic oscillator model are explained below. Synchronized oscillations with a period of about 24 hours are observed in Per mRNAs and  $\text{Ca}^{2+}$  [Fig. 5(c)]. In the second simulation the network is only composed of mutant neurons [Fig. 5(b)]. Each neuron also contains a genetic clock but due to the mutation they are uncoupled. In this second simulation, synchronized oscillations are not observed in PER proteins [Fig. 5(d), bottom]. Nevertheless,

our model predicts oscillations of  $\text{Ca}^{2+}$  [Fig. 5(d), top]. This result diverges from what would be expected of a SCN driven by genetic clocks. In a genetic clock mechanism, second messengers are only coupling agents and they cannot oscillate synchronously in a SCN with uncoupled genetic clocks. In contrast, our model predicts that uncoupling genetic clocks only reduces the period and amplitude of second messenger oscillations. In the wild-type SCN, the advantage of coupling the intercellular clock with genetic oscillators is that fewer connections among neurons are needed to obtain synchronized rhythms [Fig. 5(e)]. The difference in the  $O_p$  between wild-type and mutant neurons is clearly distinguishable in the range of 240–400 connections. For example, the mutant SCN needs 360 connections to obtain an  $O_p$  of about 0.5 and the wild type needs about 20% less, 280 connections.

In Fig. 5, we consider that neuropeptide release is affected by genetic clocks and have added the reaction [32]



where  $\text{mRNA}_j$  is the number of Per mRNAs in neuron  $j$  and  $r_6$  is the reaction rate. Therefore, there are two sources that stimulate neuropeptide release [30]: second messengers, by reaction (1), and genetic clocks, by reaction (6). These sources are denoted as II and VI in Figs. 5(a) and 5(b). The percentages of neuropeptides released by reactions (1) and (6) depend on  $r_1$  and  $r_6$ , respectively. The values of these rates for each percentage are shown in Table SVI [39]. The

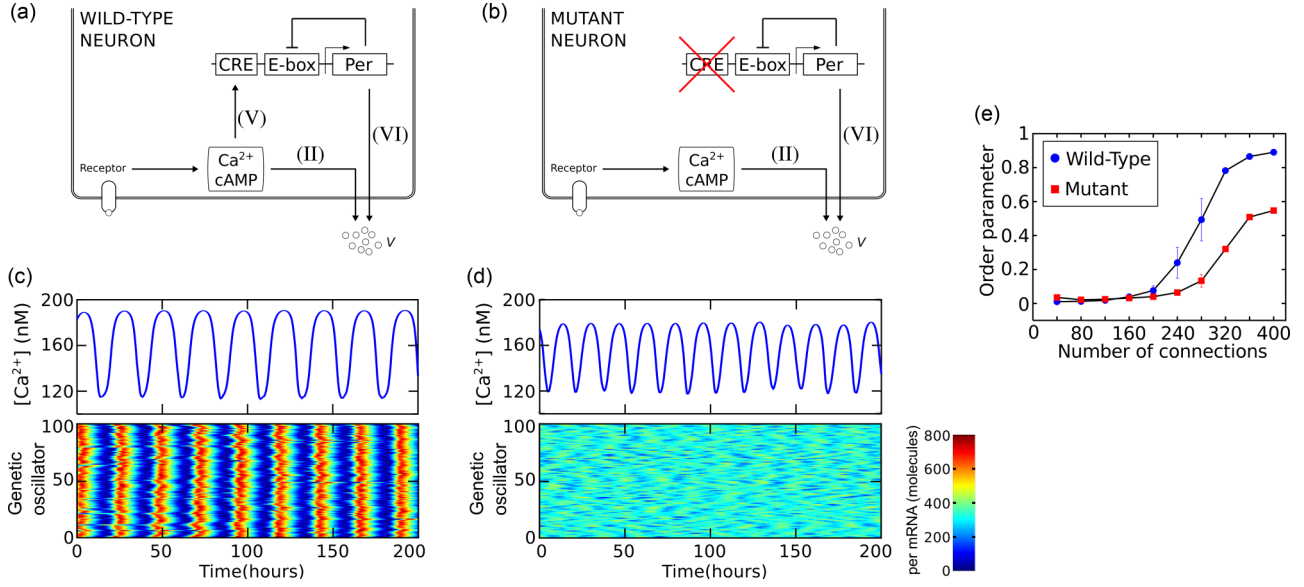


FIG. 5. (Color online) Intercellular clock coupled with genetic clocks. (a) Wild-type neuron model. Each neuron contains a genetic clock in which a gene, called *Per*, represses the activation of its promoter, called *E-box*. The transcription rate of *Per* is stimulated by  $\text{Ca}^{2+}$  through the activation of a promoter called *CRE* (V). The genetic clock stimulates neuropeptide release [30,32] (VI). (b) Mutant neuron model. The promoter *CRE* is inoperative, then the transcription of the gene is not stimulated by second messengers. This means that the genetic oscillators are uncoupled. (c) and (d) Time evolution of  $\text{Ca}^{2+}$  (top) and raster plot of time evolution of *Per* mRNA (bottom) in wild-type and mutant SCN, respectively. We scale  $m$  to calculate  $[\text{Ca}^{2+}]$  (see calculation of  $[\text{Ca}^{2+}]$  in Appendix B). (e)  $O_p$  as a function of the number of connections in wild-type (blue circle, calculated for *Per* mRNA) and mutant SCN (red square, calculated for neuropeptides). To simulate (c), (d), and (e) we used  $r_1 = 80 \text{ molecules hour}^{-1}$  and  $r_6 = 0.04 \text{ hour}^{-1}$  (see Fig. S3 and Table SVI [39]).

specific combination of percentages is not known and we have calculated the  $O_p$  for mutant SCN depending on these percentages (Fig. S3 [39]). The mutant SCN shows synchronization when 60% or more of neuropeptides are released by the stimulation of second messengers and neuropeptides. And the synchronization diminishes when the neuropeptide release mostly depends on genetic clocks.

We use a standard gene clock model that has been studied for circadian clocks in *Neurospora*, *Drosophila*, and mammals [35]. This model involves one of the main proteins expressed rhythmically in SCN neurons called *PER*. These *PER* proteins inhibit their own expression creating a negative feedback loop in the genetic clock (Fig. S2 [39]). This gene oscillator model is described by the biochemical reactions shown in Table SIV [39]. The transcription rate of *Per* mRNA is stimulated by  $\text{cAMP}$  and  $\text{Ca}^{2+}$  in wild-type neurons [21] and can be expressed as [26]

$$v_l = v_0 + cm_l, \quad (7)$$

where we assume that the basal transcription rate of *Per* mRNA ( $v_0$ ) and the induced transcription by  $\text{cAMP}$  and  $\text{Ca}^{2+}$  signaling ( $cm_l$ ) are additive. The parameter  $c$  scales the effect of the induced transcription by  $\text{cAMP}$  and  $\text{Ca}^{2+}$ . In mutant neurons, the genetic oscillators are not connected to the extracellular clock. Then, we have  $c = 0$  and the transcription rate  $v_l$  reaches its basal value  $v_0$ . We recall that isolated genetic clocks are unstable oscillators [23,24], and we choose a value for  $v_0$  that produces irregular oscillations and periods in unconnected genetic clocks (Fig. S2 [39]). In our model, second messenger activity, neuropeptide release, and nascent gene expression are crucial for the proper functioning of the

intercellular clock (Fig. 6). The abolition of these functions by drugs stops the oscillations.

#### IV. CONCLUSIONS

We have proposed and studied a model that can help to clarify the oscillatory mechanism of the SCN. We have shown that the network of neuropeptides and second messengers in the SCN can act as an intercellular clock that produces oscillations by itself. We have also shown that this result diverges from what would be expected of a master clock driven by genetic clocks. The model is robust to parameter perturbations and can be entrained by light-dark cycles. Therefore, we suggest that the SCN has taken advantage of the network of neuropeptides and second messengers to create a main circadian pacemaker rather than just connecting genetic oscillators. We expect that these findings may help us to obtain a better understanding of diseases related to circadian disturbances such as neurodegeneration, cancer, and sleep disorders.

#### ACKNOWLEDGMENTS

This work was supported by the European Regional Development Fund in the IT4Innovations Centre of Excellence project (CZ.1.05/1.1.00/02.0070) and the EU project Development of Research Capacities of the Silesian University in Opava (CZ.1.07/2.3.00/30.0007). We would also like to thank the anonymous reviewers for useful comments on the manuscript.

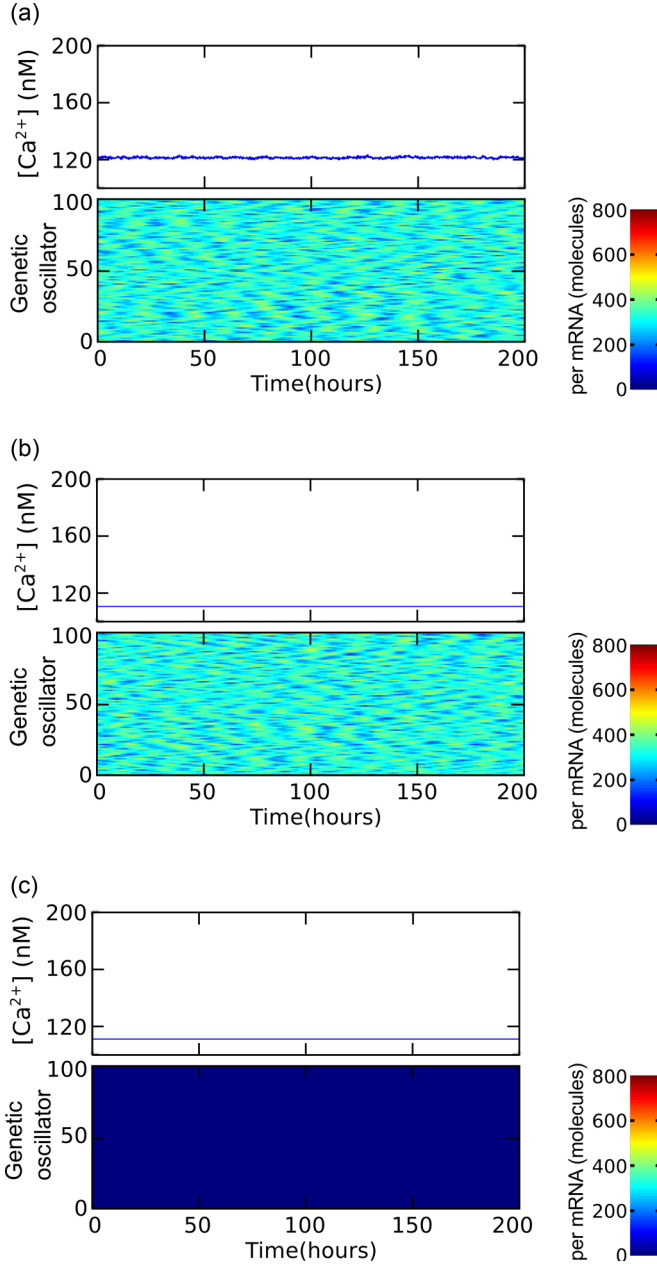


FIG. 6. (Color online) The abolition of second messenger activity, neuropeptide release, or nascent gene expression by drugs stop the oscillations in the SCN. (a) Abolition of second messenger activity. We have changed the rate in reaction (1) by  $\gamma m_j r_1$  and now  $v_i = v_0 + \gamma c m_i$ . (b) Abolition of neuropeptide release. We have changed the rates in reactions (1) and (6) by  $\gamma m_j r_1$  and  $\gamma \text{mRNA}_j r_6$ . (c) Abolition of nascent gene expression. We have changed the rate in reaction (1) by  $\gamma m_j r_1$  and now  $v_i = \gamma(v_0 + c m_i)$ . In (a), (b), and (c) the parameter  $\gamma$  takes into account the strength of the drugs in the SCN (as in [32]).  $\gamma = 1$  means no presence of drugs and  $\gamma = 0$  means presence of drugs. In (a), (b), and (c) time evolution of  $\text{Ca}^{2+}$  (top) and raster plot of time evolution of Per mRNA (bottom).

#### APPENDIX A: CALCULATION OF $m_j$

In our model, we do not distinguish between the second messengers cAMP and  $\text{Ca}^{2+}$ . We denote the second messengers by the variable  $M$ . At the steady state, the amount

of second messengers  $M_j$  in the neuron  $j$  can be written as [26]

$$k M_j = \alpha_0 + \alpha_1 \beta, \quad (\text{A1})$$

where  $k$  is the efflux or degradation rate of second messengers,  $\alpha_0$  is the influx or synthesis rate of second messengers, and  $\alpha_1$  is the influx or synthesis rate of second messengers stimulated by neuropeptides. The parameter  $\alpha_1$  is modulated by the fraction of activated receptors  $\beta$ . We use a simple model of receptor and ligand to calculate  $\beta$  [26]:

$$F_j + R_j \xrightleftharpoons[k_r]{k_f} R_j^a, \quad (\text{A2})$$

where  $F_j$  are the released neuropeptides in neuron  $j$  from the incoming connections,  $R_j$  are the receptors, and  $R_j^a$  represents the activated receptors. We assume that the number of receptors is constant in each neuron  $R_t = R_j + R_j^a$ . We also assume that the receptor-ligand dynamics are fast compared with the circadian period of the oscillations. Then

$$\beta = \frac{R_j^a}{R_t} = \frac{F_j}{K + F_j}, \quad (\text{A3})$$

where  $K = k_r/k_f$  is the equilibrium dissociation constant,  $F_j = \sum_k V_k$ , and  $V_k$  is the number of neuropeptides released to neuron  $j$  in the connection  $k$ .

Therefore, Eq. (A1) can be written as

$$M_j = \frac{\alpha_0}{k} + \frac{\alpha_1}{k} \frac{F_j}{K + F_j}. \quad (\text{A4})$$

It is useful to nondimensionalize  $M_j$  in order to obtain a parameter ( $m_j$ ) that represents the strength of the cAMP and  $\text{Ca}^{2+}$  signaling in the SCN. We obtain Eq. (4) from (A4) introducing new variables  $m_j = k M_j / (\alpha_0 + \alpha_1)$  and  $m_0 = \alpha_0 / (\alpha_0 + \alpha_1)$ .

#### APPENDIX B: CALCULATION OF $[\text{Ca}^{2+}]$

To calculate  $[\text{Ca}^{2+}]$  in the SCN we scale the strength of the cAMP and  $\text{Ca}^{2+}$  signaling to lie between  $[\text{Ca}^{2+}]_{\text{max}} = 191$  nM and  $[\text{Ca}^{2+}]_{\text{min}} = 113$  nM (values obtained from Ref. [22]). Specifically, the equation is the following:

$$[\text{Ca}^{2+}] = a \bar{m} + b,$$

where  $\bar{m} = \frac{1}{N} \sum_{j=1}^N m_j$ . The biological meaning of this equation is simply that the maximum (minimum) strength of the cAMP and  $\text{Ca}^{2+}$  signaling is reached when  $[\text{Ca}^{2+}]$  is maximum (minimum). To obtain the values of  $a$  and  $b$  we have to solve the following system of equations:

$$[\text{Ca}^{2+}]_{\text{max}} = a \bar{m}_{\text{max}} + b,$$

$$[\text{Ca}^{2+}]_{\text{min}} = a \bar{m}_{\text{min}} + b,$$

where  $\bar{m}_{\text{max}} = 0.899$  and  $\bar{m}_{\text{min}} = 0.0323$  were obtained from simulation of wild-type SCN. The solution is  $a = 90$  nM and  $b = 110$  nM.

- [1] J. A. Mohawk, C. B. Green, and J. S. Takahashi, *Annu. Rev. Neurosci.* **35**, 445 (2012).
- [2] C. S. Colwell, *Nat. Rev. Neurosci.* **12**, 553 (2011).
- [3] A. A. Kondratova and R. V. Kondratov, *Nat. Rev. Neurosci.* **13**, 325 (2012).
- [4] M. W. Greene, *Cancer Lett.* **318**, 115 (2012).
- [5] D. K. Welsh, J. S. Takahashi, and S. A. Kay, *Annu. Rev. Physiol.* **72**, 551 (2010).
- [6] B. C. Goodwin, *Adv. Enzyme Regul.* **3**, 425 (1965).
- [7] A. Goldbeter, *Proc. R. Soc. B* **261**, 319 (1995).
- [8] N. Barkai and S. Leibler, *Nature (London)* **403**, 267 (2000).
- [9] W. Mather, M. R. Bennett, J. Hasty, and L. S. Tsimring, *Phys. Rev. Lett.* **102**, 068105 (2009).
- [10] J. M. Miró-Bueno and A. Rodríguez-Patón, *PLoS ONE* **6**, e27414 (2011).
- [11] J. C. Leloup and A. Goldbeter, *Proc. Natl. Acad. Sci. USA* **100**, 7051 (2003).
- [12] D. B. Forger and C. S. Peskin, *Proc. Natl. Acad. Sci. USA* **100**, 14806 (2003).
- [13] H. P. Mirsky, A. C. Liu, D. K. Welsh, S. A. Kay, and F. J. Doyle, *Proc. Natl. Acad. Sci. USA* **106**, 11107 (2009).
- [14] T. Y. Tsai, Y. S. Choi, W. Ma, J. R. Pomeroy, C. Tang, and J. E. Ferrell, *Science* **321**, 126 (2008).
- [15] J. Hasty, M. Dolnik, V. Rottschäfer, and J. J. Collins, *Phys. Rev. Lett.* **88**, 148101 (2002).
- [16] H. Kori and A. S. Mikhailov, *Phys. Rev. Lett.* **93**, 254101 (2004).
- [17] M. C. Harrisingh, Y. Wu, G. A. Lnenicka, and M. N. Nitabach, *J. Neurosci.* **27**, 12489 (2007).
- [18] J. S. O'Neill, E. S. Maywood, J. E. Chesham, J. S. Takahashi, and M. H. Hastings, *Science* **320**, 949 (2008).
- [19] M. H. Hastings, E. S. Maywood, and J. S. O'Neill, *Curr. Biol.* **18**, R805 (2008).
- [20] C. H. Ko, Y. R. Yamada, D. K. Welsh, E. D. Buhr, A. C. Liu, E. E. Zhang, M. R. Ralph, S. A. Kay, D. B. Forger, and J. S. Takahashi, *PLoS Biol.* **8**, e1000513 (2010).
- [21] J. S. O'Neill and A. B. Reddy, *Biochem. Soc. Trans.* **40**, 44 (2012).
- [22] M. Brancaccio, E. S. Maywood, J. E. Chesham, A. S. Loudon, and M. H. Hastings, *Neuron* **78**, 714 (2013).
- [23] J. A. Mohawk and J. S. Takahashi, *Trends Neurosci.* **34**, 349 (2011).
- [24] J. B. Hogenesch and E. D. Herzog, *FEBS Lett.* **585**, 1427 (2011).
- [25] D. Gonze, S. Bernard, C. Waltermann, A. Kramer, and H. Herzel, *Biophys. J.* **89**, 120 (2005).
- [26] T.-L. To, M. A. Henson, E. D. Herzog, and F. J. Doyle III, *Biophys. J.* **92**, 3792 (2007).
- [27] S. Bernard, D. Gonze, B. Čajavec, H. Herzel, and A. Kramer, *PLoS Comput. Biol.* **3**, e68 (2007).
- [28] E. Ullner, J. Buceta, A. Díez-Noguera, and J. García-Ojalvo, *Biophys. J.* **96**, 3573 (2009).
- [29] C. Vasalou, E. D. Herzog, and M. A. Henson, *J. Biol. Rhythms* **24**, 243 (2009).
- [30] C. Vasalou and M. A. Henson, *PLoS Comput. Biol.* **6**, e1000706 (2010).
- [31] C. Vasalou, E. D. Herzog, and M. A. Henson, *Biophys. J.* **101**, 12 (2011).
- [32] M. Hafner, H. Koepl, and D. Gonze, *PLoS Comput. Biol.* **8**, e1002419 (2012).
- [33] M. A. Henson, *Chaos, Solitons Fractals* **50** 48 (2013).
- [34] B. Ananthasubramaniam, E. D. Herzog, and H. Herzel, *PLoS Comput. Biol.* **10**, e1003565 (2014).
- [35] D. Gonze and A. Goldbeter, *Chaos* **16**, 026110 (2006).
- [36] J. F. McKelvy and S. Blumberg, *Annu. Rev. Neurosci.* **9**, 415 (1986).
- [37] W. G. Regehr, M. R. Carey, and A. R. Best, *Neuron* **63**, 154 (2009).
- [38] E. Sel'Kov, *Eur. J. Biochem.* **4**, 79 (1968).
- [39] See Supplemental Material at <http://link.aps.org/supplemental/10.1103/PhysRevE.90.032705> for details .
- [40] P. Smolen, D. A. Baxter, and J. H. Byrne, *J. Neurosci.* **21**, 6644 (2001).
- [41] M. C. Antle and R. Silver, *Trends Neurosci.* **28**, 145 (2005).
- [42] D. T. Gillespie, *J. Phys. Chem.* **81**, 2340 (1977).
- [43] J. Garcia-Ojalvo, M. B. Elowitz, and S. H. Strogatz, *Proc. Natl. Acad. Sci. USA* **101**, 10955 (2004).